

Article

Not peer-reviewed version

Determination Mitochondria's Quality Control of Parkinsonism Using Real-Time Reverse-Transcription Polymerase Chain Reaction

[Al-Baraa Akram](#) *

Posted Date: 28 April 2024

doi: 10.20944/preprints202404.1845.v1

Keywords: RT: real time, PCR: polymerase chain reaction, WT: wild type, dNTP: deoxynucleotide triphosphate



Preprints.org is a free multidiscipline platform providing preprint service that is dedicated to making early versions of research outputs permanently available and citable. Preprints posted at Preprints.org appear in Web of Science, Crossref, Google Scholar, Scilit, Europe PMC.

Copyright: This is an open access article distributed under the Creative Commons Attribution License which permits unrestricted use, distribution, and reproduction in any medium, provided the original work is properly cited.

Article

Determination Mitochondria's Quality Control of Parkinsonism Using Real-Time Reverse-Transcription Polymerase Chain Reaction

Al-Baraa Akram

Faculty of health and life science, De Montfort University-Leicester, United Kingdom;
albraaakram94@gmail.com; Tel.: (+16469631415)

Abstract: Nuclear DNA mutations, mitochondrial DNA mutations, combined nuclear and mitochondrial DNA defects, and random occurrences are the main causes of mitochondrial disease. Black pigmentation loss is a major sign of Parkinsonism. Because of the loss of dopaminergic neurons in the substantia nigra, it drops to less than 80%. The degree of motor impairment was correlated with the amount of black pigmentation loss. After RNA extraction, reverse transcription is carried out because reverse transcriptase was used to create cDNA. One microliter of total RNA supplemented with IORT Buffer, dNTPs, random hexamers, Multi-Scribe Reverse Transcriptase, and nuclease-free was used to create cDNA. The following was how the reaction was carried out in a thermal cycler: 10 minutes at 25°C, 120 minutes at 37°C, 5 seconds at 85°C, and lastly 4°C. The data was expressed as a v-value, which shows how much the target gene is enriched in comparison to the reference gene. Earlier research using mice injected with functional HtrA2/Omi protease activity revealed similar outcomes, including induced up-regulation of CHOP, decreased mitochondrial function, and early brain cell aging because of an increase in mtDNA deletions. The cell viability of the genotypes exhibits a dmg concentration-dependent effect in these results, suggesting that high content ratios of drug treatment with 6-OHDA may be the cause of cellular content depletion. After 6-OHDA neurotoxin treatment, CHOP is up-regulated. Prior in vitro research has shown that treatment with a model based on 6-OHDA neurotoxin causes the activation of mitochondrial stress pathways, which in turn promotes the death of neurons. 6-OHDA reversibly inhibited complexes I and IV's activities in rat brain cells, which led to dopaminergic neurodegeneration, a defining feature of PD pathogens. As a result, the number of living cells will directly correlate with the dmg concentration, supporting the results of the current study. Real-time PCR can generally demonstrate that the removal of HtrA 2 results in a significant up-regulation of Hsp60 expression when compared to WT cells. This could be linked to a decreased threshold for mitochondrial stress in HtrA2 KO cells, which would explain why, following ADEP4 and ACP5 treatment, Hsp60 is significantly up-regulated in HtrA2 KO cells compared to WT cells.

Keywords: RT: real time; PCR: polymerase chain reaction; WT: wild type; dNTP: deoxynucleotide triphosphate

1. Introduction

Function and survival of dopaminergic neurons strongly rely on appropriate mitochondrial homeostasis. Mitochondrial dysfunction has been widely accepted as one of the major pathogenic pathways underlying the development of PD (1). Mitochondrial matrix prevents polypeptides aggregation and assists in correct protein folding; moreover prevent the accumulation of harmful oxygen species. This mechanism of molecular quality control represents a form of mitochondrial transcriptional response program known as mitochondrial unfolded protein response (mtUPR) (2). Fusion and fission dynamics ensure normal mitochondrial morphology and functions with a minimal release of ROS. Overexpression of fusion and fission processes decrease energy production due to limitations in mitochondrial motility, thus increases continuous oxidative stress, which promotes cell

dysfunction and later cell death. Dysfunction of mitochondria quality control results in accumulation of impaired mitochondria and consequently increases the number of harmful oxygen species involved in dopaminergic neuro-degeneration (3).

HtrA2, also known as Omi, encodes a highly conserved mitochondrial localized serine protease that is part of the high-temperature requirement factor A (HtrA) family. Due to its structural conformation, HtrA2 proteases can enable the activation or coordinate an array of signaling pathways implicated in PQC. Impairment of HtrA2 proteolytic activity leads to aggregation of unfolded proteins within mitochondria, impairment of the mitochondrial respiration and augmented production of ROS giving rise to disequilibrium of mitochondrial bioenergetics (4).

Parkinson's Disease Neuropathology

It is characterized by severe loss of black pigmentation (neuromelanin). It decreases to less than 80% due to dopaminergic neuronal loss in substantia nigra (pars compacta). Degree of loss of black pigmentation correlated with degree of motor impairment.

The clinical features ranging between 60% to 80% dopaminergic neurons loss. Other brain areas are affected: e.g locus ceruleus, raphe cortex. It is known by appearance of abnormal cytoplasmic bodies in brain tissue (Lewy bodies).

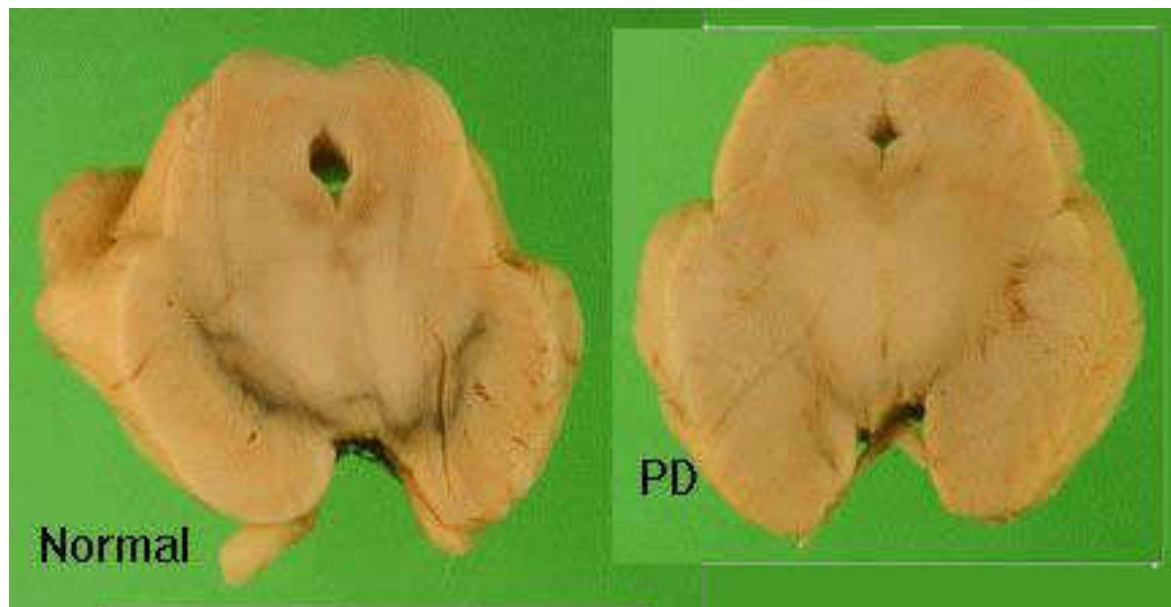


Figure 1. Post-mortem brain section showing loss of black pigmentation in substantia nigra in PD.

Anatomy of Dopaminergic Neurons

Dopamine is most abundant in corpus striatum which is involved in coordination of movement including frontal cortex, limbic system and hypothalamus. Nigrostriatal Pathway (cell bodies in Substantia Nigra with projections to striatum. Mesolimbic pathway starts in Ventral Tegmental Area and projects in the limbic system (amygdala and Nucleus accumbens) as Mesocortical Pathway from VTA to frontal cortex. Tuberohypophyseal pathway controls pituitary gland.

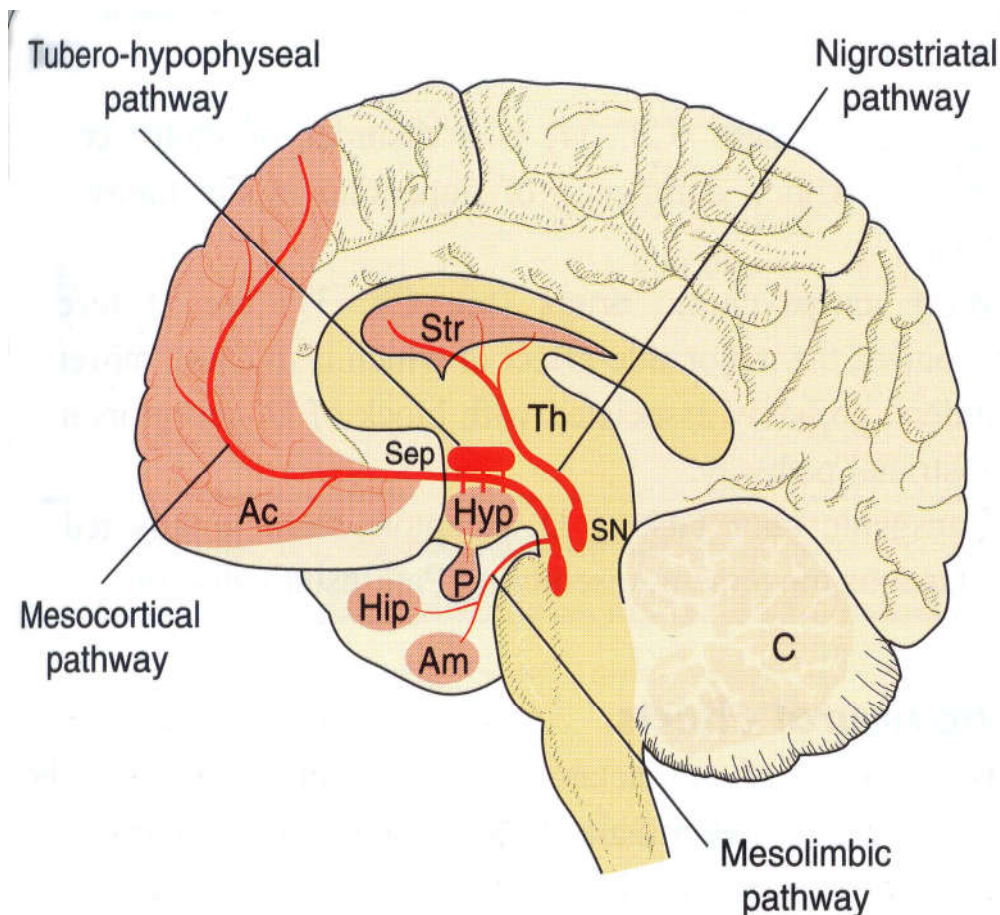


Figure 2. Dopaminergic Neuron Anatomy showing nigrostriatal pathway, tubero-hypophyseal pathway, mesolimbic pathway and mesocortical pathway.

Parkinson's Disease Clinical Presentation

Tremors: It is one of the most distinct clinical presentations is resting tremors; it may remain the predominant syndrome for several years. It is characterized by reduction with activity, tremors increase with walking, anxious and heat sensation.

Resting tremors between 4-6 Hz usually start first in finger, basically thumb, and may affect also the legs, mouth and tongue. Tremors involve coarse, complex movements, flexion/extension of fingers. It can be specified with adduction and abduction of the thumb and supination and pronation of forearm. It may affect arms, legs, feet, jaw and tongue which can be intermittent, present at rest and during distraction.

Postural tremors between 8-10 Hz are less obvious and have finer amplitude. It present on action or posture and persists with movement.

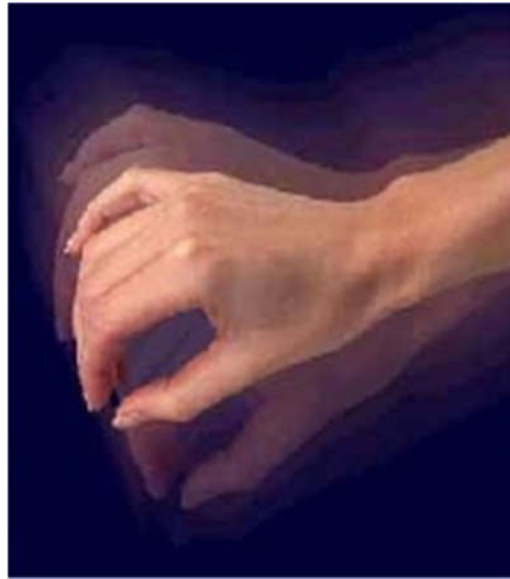


Figure 3. 4-6 Hz resting tremors typically begin in the finger, primarily the thumb.

2. Materials and Methods

Reverse Transcription

RNA-dependent DNA polymerase enzymes called reverse transcriptases (RTs) were first identified from retroviruses. Reverse transcription-using dsRNA viruses, including the hepatitis B virus, and other retro-elements in prokaryotes and eukaryotes code for RTs. Reverse transcriptases include the enzyme telomerase, which keeps the ends of eukaryotic chromosomes intact. However, telomerase functions substantially differently from traditional RTs in terms of how it works. The discovery of RT transformed molecular biology, causing the core theories to be rewritten and allowing researchers to create new instruments that had a significant impact on RNA biology, gene expression studies, and cloning.

RNAse H endonuclease selectively breaks down the RNA strand of DNA/RNA hybrids; RNA-dependent DNA polymerase activity that turns single-stranded cDNA into dsDNA; and ssRNA template and primer to create ssDNA/cDNA, which stays hybridized to its RNA template. Traditional RT enzymes contain two active sites, one of which is responsible for endonuclease activity and the other for polymerase activity. Certain RT proteins are dimeric or monomeric, and they don't have intrinsic RNAse H activity. To improve thermo-stability and modulate RNAseH activity, those enzymes have been optimized through the use of site-directed mutagenesis and protein evolution. Reducing the influence of complex secondary structures and reducing nonspecific nucleic acid amplification are two advantages of using the thermostable variant of RT.

While decreased RNAseH activity is advantageous in cDNA cloning methods, particularly when reverse transcribed very lengthy mRNA transcripts, robust RNAseH activity is advantageous in RT-PCR. In certain instances, RT is simply utilized to create the RNA/DNA hybrid; the polymerization of cDNA to dsDNA is done by a traditional DNA pol.

After RNA extraction, cDNA was synthesized with reverse transcriptase. cDNA was synthesized from 1 µl total RNA (50 ng/µL) containing 2.0 µl IORT Buffer (Applied Bio Systems), 0.8 µl 25X dNTPs, 2.0 µl 10X random hexamers, 0.5 µl Multi-Scribe Reverse Transcriptase and 4.7 µl nuclease free. The reaction was performed in a Thermal Cycler as follows: 25° C for 10 min, 37° C for 120 min, 85° C for 5 sec and finally 4° C.

Real-Time RT-PCR

Real-time PCR was performed in an Applied Bio-systems thermo-cycler using SYBR green PCR master mix detection according to the manufacture's protocol. The following PCR conditions were

used: 50° C for 2 min, 95° C for 10 min, and 40 cycles of 95° C for 15 seconds and 60° C for 1 min. The following primers were used: mouse ATG5 (Forward primer: 5-AACTGAAAGAG AAGCAGAACCA-3; reverse primer: 5-TGTCTCAT AACCTTCTGAAAGTGC-3); mouse Hsp 60 (Forward primer: 5-GCCTTAATGCTTCAAGGTGTAGA-3; reverse primer: 5-CCCCATCTTTTGTTACTTTGGA-3). The data was reported as v-value, representing the enrichment of the target gene relative to the reference gene (5).



Figure 4. Comparison of human HtrA2/Omi protein sequence with several other eukaryotic species. Clustal Omega multiple sequence analysis showed high sequence conservation in the Trypsin and PDZ domains of the analyzed species. Asterisks (*) indicate the residues that are identical, colons (:) indicate the conserved substitutions, and periods (.) indicate the semi-conserved substitutions.

Accession number of human HTRA2 mitochondrial isoform 1 preproprotein [Homo sapiens]:
NM_013247.5

The gene sequence is

CTACTGTCCGCTGCTCGCGTCCTGGGTGCCGCCTCTGAGTAGGGCGGGCGAGGAGGC
AGCCAAGGCGGAGCTGATGGCTGCGCCGAGGGCGGGGCGGGGTGCAGGCTGGAGCCTTCG
GGCATGGCGGGCTTTGGGGGGCATTGCTGGGGGAGGAGACCCCGTTTGACCCCTGACCTC
CGGGCCCTGCTGACGTCAGGAATTCTGACCCCCGGGCCCGAGTGACTTATGGGACCCCCA
GTCTCTGGGCCCCGTTGTCTGTTGGGGTCACTGAACCCGAGCATGCCTGACGTCTGGGACC
CCGGGTCCCCGGGCACAACCTGACTGCGGTGACCCAGATACCAGGACCCGGGAGGCCTCA

GAGAACTCTGGAACCCGTTCCGCGCGCTGGCTGGCGGTGGCGCTGGGCGCTGGGGGGGCA
 GTGCTGTTGTTGTTGTGGGGCGGGGGTTCGGGGTCTCTCCGGCCGTCCTCGCCGCCGTCCTAG
 CCCGCCGCCGCTTCTCCCCGAGTCAGTACAACCTTCATCGCAGATGTGGTGGAGAAGACA
 GCACCTGCCGTGGTCTATATCGAGATCCTGGACCGGCACCCTTTCTTGGGCCGCGAGGTCCC
 TATCTCGAACGGCTCAGGATTCGTGGTGGCTGCCGATGGGCTCATTTGTACCAACGCCCAT
 GTGGTGGCTGATCGGCGCAGAGTCCGTGTGAGACTGCTAAGCGGCGACACGTATGAGGCC
 GTGGTCACAGCTGTGGATCCCGTGGCAGACATCGCAACGCTGAGGATTCAGACTAAGGAG
 CCTCTCCCCACGCTGCCTCTGGGACGCTCAGCTGATGTCCGGCAAGGGGAGTTTGTGTTGC
 CATGGGAAGTCCCTTTGCACTGCAGAACACGATCACATCCGGCATTGTTAGCTCTGCTCAG
 CGTCCAGCCAGAGACCTGGGACTCCCCCAAACCAATGTGGAATACATTCAAACCTGATGCA
 GCTATTGATTTTGGAACTCTGGAGGTCCCCTGGTTAACCTGGATGGGGAGGTGATTGGAGT
 GAACACCATGAAGGTCACAGCTGGAATCTCCTTTGCCATCCCTTCTGATCGTCTTCGAGAGT
 TTCTGCATCGTGGGGAAAAGAAGAATTCCTCCTCCGGAATCAGTGGGTCCCAGCGGCGCTA
 CATTGGGGTGTGATGCTGACCCTGAGTCCCAGCATCCTTGCTGAACTACAGCTTCGAGAA
 CCAAGCTTTCCCGATGTTTACAGCATGGTGTACTCATCCATAAAGTCATCCTGGGCTCCCCTGC
 ACACCGGGCTGGTCTGCGGCCTGGTGTGATGTTTGGCCATTGGGGAGCAGATGGTACAA
 AATGCTGAAGATGTTTATGAAGCTGTTTGAACCCAATCCCAGTTGGCAGTGCAGATCCGGC
 GGGGACGAGAAACACTGACCTTATATGTGACCCCTGAGGTCACAGAATGAATAGATCACC
 AAGAGTATGAGGCTCCTGCTCTGATTTCTCCTTGCCCTTCTGGCTGAGGTTCTGAGGGCAC
 CGAGACAGAGGGTTAAATGAACAGTGGGGGCAGGTCCCTCCAACCACCAGCACTGACTC
 CTGGGCTCTGAAGAATCACAGAAACACTTTTTATATAAAATAAAATTATACCTAGCAACAT
 ATTATAGTAAAAAATGAGGTGGGAGGGCTGGATCTTTTCCCCCACCAAAGGCTAGAGGTA
 AAGCTGTATCCCCCTAAACTTAGGGGAGATACTGGAGCTGACCATCCTGACCTCCTATTAA
 AGAAAATGAGCTGCTGCCA

Serine protease HTRA2, mitochondrial [Mus musculus]

NCBI Reference Sequence: NM_019752.3

The gene sequence is

CTGGAGAGGAGCGCGTCCTGACGGGACTACGTTTCCCGGCATGCGCTGAACAGCTACC
 GTCGTGCCCTGCTTCTCCTAGACCGCTTGCCGGGTTCTAGAGGACCGCCTCTGAGTAGGGCG
 GCGGAGGAGAGTCGAGGCGGAGCTGATGGCTGCGCTGAAAGCGGGGCGGGGTGCAAACCT
 GGAGCCTTCGGGCATGGCGGGCTTTGGGGGGCATCTTCTGGAGGAAGCCTCCCCTGTTAGC
 TCCTGACCTCCGGGCTCTGCTGACGTCAGGAACCTGACTCTCAGATCTGGATGACTTATG
 GGACCCCCAGTCTCCCGGCCAGGTGCCTGAGGGGTTCTTGCATCACGGGCAGATCTGAC
 GTCTAGGACCCCGGATCTCTGGGCACGATTGAATGTGGGGACTTCAGGCTCCAGTGACCAG
 GAGGCCCCGAGGAGCCCTGGAAGCCGTCGGCGCGAATGGCTGGCGGTGGCGGTGGGCGCA
 GGAGGTGCAGTGGTGTGCTGTTGTGGGGTTGGGGTCGGGGTCTTTCCACGGTGCTGGCTGC
 GTTTCCTGCTCCGCCACCCACTTCTCCCCGAGCCAGTACAATTCATCGCAGATGTGGTGG
 AGAAGACAGCCCCTGCTGTGGTCTATATCGAGATCCTAGACCGGCACCCTTTCTCCGGCCG
 TGAAGTCCCCATCTCAAACGGATCAGGATTCGTAGTGGCTTCAGATGGGCTCATCGTTACC
 AACGCCCCAGTGGTGGCTGATCGGCGCCGAGTACGAGTGGGCTGCCTAGCGGGGATACTT
 ATGAGGCCATGGTCACAGCTGTGGATCCCGTAGCAGACATTGCCACACTGAGGATTCAAAC
 CAAGGAGCCTCTTCCCACACTGCCCTCGGCCGCTCTGCTGATGTCCGGCAAGGGGAGTTT
 GTTGTGTCATGGGAAGCCCCCTTTGCACTGCAGAACACGATCACATCTGGTATTGTCAGCTC
 TGCTCAGCGCCCAGCCAGGGACCTGGGACTCCCTCAAAACAACGTGGAATACATTCAGAC
 CGATGCAGCTATTGATTTTGGAAATTCGGTGGTCCCCTGGTTAACCTGGATGGGGAGGTGA
 TTGGAGTGAACACCATGAAGGTGACAGCTGGAATCTCCTTTGCCATCCCTTCTGATCGCCTT
 AGGGAGTTTCTGCATCGCGGGGAAAAGAAAAAATTCCTGGTTTGGAAACAGTGGGTCCCAGC
 GCCGCTACATTGGAGTGATGATGCTGACCCTGACTCCCAGCATCCTTATTGAACTACAGCTC
 CGTGAGCCAAGCTTCCCTGATGTTTACAGCATGGTGTCTCATTCATAAAGTTATCCTGGGCTC
 CCCCCACACAGGGCTGGTCTGCGGCCTGGTGTGATGTTTGGCCATTGGGGAGAAATTG
 GCACAAAATGCTGAAGATGTTTATGAAGCTGTTTGAACCCAATCACAGCTGGCAGTGCGGA
 TCCGGCGCGGATCAGAGACACTGACCTTATATGTGACCCCCGAGGTCACAGAATGAATGA

CTGGACCGGCAAGAGTGTGAAGCTCTTGCCCTGATCTCCTCCTTGCTTTCCTAGCCTAGGTT
CTGAGTGCATGTGGGTAGAGGAGGAGTCAGTGAACCTGCGGAGGGCAAGTCCCTCTAACC
GCTGCATCAGTCCTGGGCTCCGAAGAACACATTTTATATAAAATAAAATTATACCTAGCAA
CATGTTACAGTCAAAAAAAAAAAAAAAAAAAAAA

TLS-CHOP [Homo sapiens] accession number: S62138.1

The gene sequence is

ATGCTCAGTCCTCCAGGCGTCGGTGCTCAGCGGTGTTGGAACCTTCGTTGCTTGCTTGCC
TGTGCGCGCGTGC GCGGACATGGCCTCAAACGATTATACCCAACAAGCAACCCAAAGCTA
TGGGGCCTACCCACCCAGCCCGGGCAGGGCTATTCCCAGCAGAGCAGTCAGCCCTACGG
ACAGCAGAGTTACAGTGGTTATAGCCAGTCCACGGACACTTCAGGCTATGGCCAGAGCAG
CTATTCTTCTTATGGCCAGAGCCAGAACACAGGCTATGGAACCTCAGTCAACTCCCCAGGGA
TATGGCTCGACTGGCGGCTATGGCAGTAGCCAGAGCTCCCAATCGTCTTACGGGCAGCAGT
CCTCCTACCCTGGCTATGGCCAGCAGCCAGCTCCCAGCAGCACCTCGGGAAGTTACGGTAG
CAGTTCTCAGAGCAGCAGCTATGGGCAGCCCCAGAGTGGGAGCTACAGCCAGCAGCCTAG
CTATGGTGGACAGCAGCAAAGCTATGGACAGCAGCAAAGCTATAATCCCCCTCAGGGCTA
TGGACAGCAGAACCAGTACAACAGCAGCAGTGGTGGTGGAGGTGGAGGTGGAGGTGGAG
GTA ACTATGGCCAAGATCAATCCTCCATGAGTAGTGGTGGTGGCAGTGGTGGCGGTTATGG
CAATCAAGACCAGAGTGGTGGAGGTGGCAGCGGTGGCTATGGACAGCAGGACCGTGGAGG
CCGCGGCAGGGGTGGCAGTGGTGGCGGCGGCGGCGGCGGCGGTGGTGGTTACAACCGCAG
CAGTGGTGGCTATGAACCCAGAGGTCTGAGGTGGCCGTGGAGGCAGAGGTGGCATGGG
CGGAAGTGACCGTGGTGGCTTCAATAAAATTTGGTGTGTTCAAGAAGGAAGTGTATCTTCAT
ACATCACCACACCTGAAAGCAGATGTGCTTTTCCAGACTGATCCAACCTGCAGAGATGGCAG
CTGAGTCATTGCCTTTCTCCTTCGGGACACTGTCCAGCTGGGAGCTGGAAGCCTGGTATGAG
GACCTGCAAGAGGTCTGTCTTCAGATGAAAATGGGGGTACCTATGTTTCACCTCCTGGAA
ATGAAGAGGAAGAATCAAAAATCTTCACCACTCTTGACCCTGCTTCTCTGGCTTGGCTGACT
GAGGAGGAGCCAGAACCAGCAGAGGTCAACAAGCACCTCCCAGAGCCCTCACTCTCCAGAT
TCCAGTCAGAGCTCCCTGGCTCAGGAGGAAGAGGAGGAAGACCAAGGGAGAACCAGGAA
ACGGAACAGAGTGGTCATTCCCCAGCCCGGGCTGGAAAGCAGCGCATGAAGGAGAAAG
AACAGGAGAATGAAAGGAAAGTGGCACAGCTAGCTGAAGAGAATGAACGGCTCAAGCAG
GAAATCGAGCGCCTGACCAGGGAAGTAGAGGCGACTCGCCGAGCTCTGATTGACCGAATG
GTGAATCTGCACCAAGCATGAACAATTGGGAGCATCAGTCCCCCACTTGGGCCACACTACC
CACCTTTCCCAGAAGTGGCTACTGACTACCCTCTCACTAGTGCCAATGATGTGACCCTCAAT
CCCACATACGCAGGGGGAAGGCTTGGAGTAGACAAAAGGAAAGGTCTCAGCTTGTATATA
GAGATTGTACATTTATTTATTACTGTCCCTATCTATTAAAGTGACTTTCTATG

DNA damage-inducible transcript 3 protein [Mus musculus]

NCBI Reference Sequence: NM_001290183.1

GGTCAGTTATCTTGAGCCTAACACGTCGATTATATCATGTTGAAGATGAGCGGGTGGC
AGCGACAGAGCCAGAATAACAGCCGGAACCTGAGGAGAGAGAACCTGGTCCACGTGCAG
TCATGGCAGCTGAGTCCCTGCCTTTACCTTGGAGACGGTGTCCAGCTGGGAGCTGGAAGC
CTGGTATGAGGATCTGCAGGAGGTCTGTCTCAGATGAAATTGGGGGCACCTATATCTCA
TCCCCAGGAAACGAAGAGGAAGAATCAAAAACCTTCACTACTCTTGACCCTGCGTCCCTAG
CTTGGCTGACAGAGGAGCCAGGGCCAACAGAGGTACACGCACATCCCAAAGCCCTCGCT
CTCCAGATTCCAGTCAGAGTTCTATGGCCCAGGAGGAAGAGGAGGAAGAGCAAGGAAGA
ACTAGGAAACGGAAACAGAGTGGTCAGTGCCCAGCCCGGCCTGGGAAGCAACGCATGAA
GGAGAAGGAGCAGGAGAACGAGCGGAAAGTGGCACAGCTAGCTGAAGAGAACGAGCGG
CTCAAGCAGGAAATCGAGCGCCTGACCAGGGAGGTGGAGACCACACGGCGGGCTCTGATC
GACCGCATGGTCAGCCTGCACCAAGCATGAACAGTGGGCATCACCTCCTGTCTGTCTCTCC
GGAAGTGTACCCAGCACCATCGCGCCAGCGCCAAGCATGTGACCCTGCACTGCACTGCAC
ATGCTGAGGAGGGGACTGAGGGTAGACCAGGAGAGGGCTCGGCTTGACATAGACGGTAC
ATTGTTTATTACTGTCCATGTCCAGTAAAGTGACTTTGTGTCAACAAAAAAAAAAAAAAAAAA
AA

Cell Viability Assay

Cell viability was assessed by the colorimetric MTT (3-(4,5- dimethylthiazolyl-2)-2,5-diphenyltetrazolium bromide) assay. Briefly, cells were plated in 96-well culture plates at a density of 10000 cells/ well. The plates were prepared for each genotype and were incubated at 37° C for 24 hours. After incubation, the genotypes were treated with DMSO (vehicle), ADP4 and ACP5 (acid phosphatase 5, 0.5 μ M). The cells were also treated with 6-hydroxyl dopamine (6-OHDA, 50 μ M) to produce the PD type phenotypes. Subsequently, the plates were visualized microscopically to obtain live cell images.

The MTT assay was performed using the Vybran MTT Cell Proliferation Assay Kit, Thermo Fisher Scientific, after drug treatment, 30 μ L of MTT solution was added and incubated for 2 hours. The 12 mM MTT reagent was prepared by adding 3 mL of PBS in to 15 mg of MTT and dissolving into 30 ml of media. Then medium was removed, and cells were re-suspended in 100 μ L of DMSO incubated at 37° C for 10 minutes. The absorbance was measured using a SpectraMax (MS) spectrophotometer at a wave length of 570 nm.

3. Results

Real-Time RT-PCR

RT-PCR analysis illustrated that depletion of HtrA 2 results in significant up-regulation of Hsp60 expression as compared to WT cells. This could be correlated with a reduction in the threshold for mitochondrial stress in HtrA2 KO cells, leading to an up-regulation of the Hsp60 that is much more reduced in HtrA2KO cells as compared to WT cells following treatment with ADEP4 and ACP5.

In cells lacking CHOP, the transcription factor that intermediates the mitochondrial stress signaling, up-regulation of Hsp60 following the treatments with ADEP4 and ACP5 is completely abolished. The transcriptional activation of mitophagy as measured by the levels of Atg5 appears to be strongly affected by both loss of HtraA2 and loss of CHOP as shown by the absence of Atg5 up-regulation by ADEP4 and ATG5 in these cell lines while the WT cells are showing the activation of signaling pathway following the mitochondrial stress treatments.

C/EBP Family of Transcription Factors

Similar results have been found in previous studies where mice injected with functional HtrA2/Omi protease activity showed induced up-regulation of CHOP, reduced mitochondrial function and premature age in brain cells, due to an increase in mtDNA deletions (6).

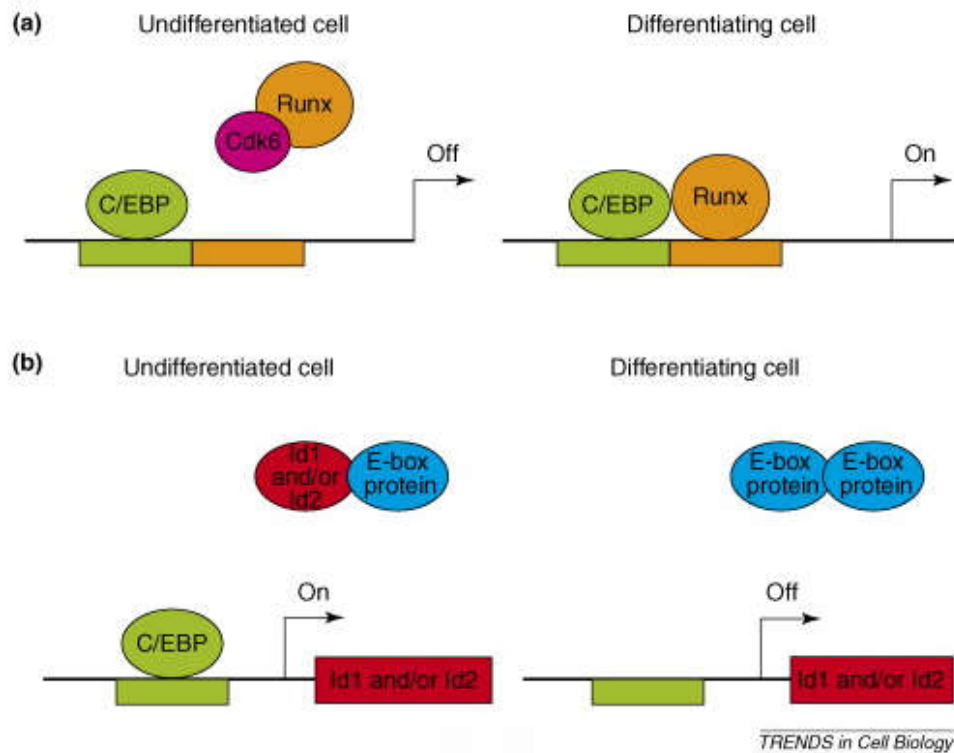


Figure 5. Schematic design of the C/EBP Family of Transcription Factors. CHOP structure comprises an N-terminal domain sequence and a bZIP domain Adapted from Wedel and Ltlmsziegler- Heil brock (1995).

4. Discussion

Suppression of both HtrA2 and CHOP is therefore likely to create a forward amplification loop, with further mitochondrial dysfunction which fails to remove the excess of oxidized and impaired protein species leading to further ROS generation. Similarly to inhibition of complex I, the presence of a positive loop in mitochondrial impairment increases the formation of ROS which can damage mitochondrial DNA (mtDNA) and other components of the PQC, contributing to mitochondrial oxidative stress and neurodegeneration.

These results display a dmg concentration-dependent effect in the cell viability of the genotypes, indicating that depletion of cellular content might be due to high content rations of drug treatment with 6-OHDA. CHOP is up-regulated upon treatment with 6-OHDA neurotoxin (7). Previous in-vitro studies have demonstrated that treatment with 6-OHDA neurotoxin-based model induced activation of mitochondrial stress pathways and promote neuronal cell death. In rat brain cells, 6-OHDA reversibly inhibited the activities of complexes I and IV, resulting in dopaminergic neurodegeneration, a hallmark of PD pathogens is (8). Therefore, the concentration of the dmg will be directly proportional to the number of living cells, corroborating to the findings in the present research.

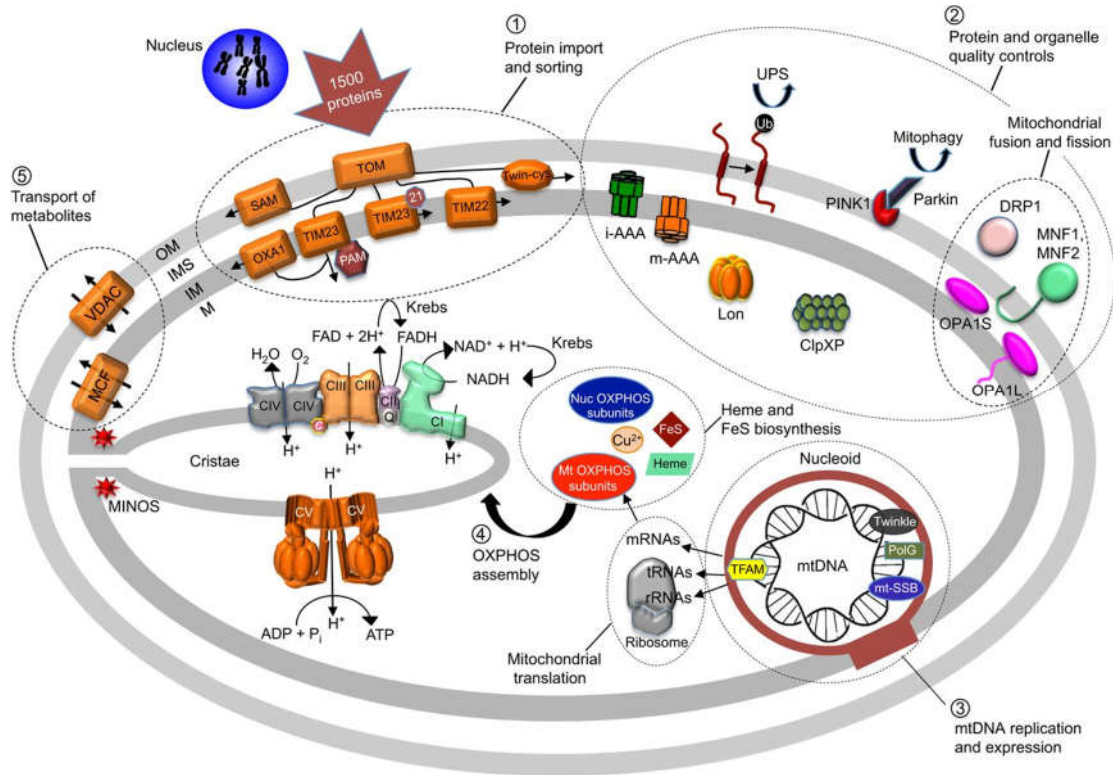


Figure 6. Summary of mitochondria's structure, function and quality control.

The main causes of mitochondrial disease are:

- nuclear DNA mutation (inherited or acquired)
- mitochondrial DNA mutation (inherited or acquired)
- Combined nuclear and mitochondrial DNA defects
- Random occurrences

Table 1. Illustrating features of mtDNA mutations vs. nuclear DNA mutations.

Feature	mtDNA mutations	Nuclear DNA mutations
Mode of inheritance	Maternal	Mendelian
Age of onset	Adults	Infancy / childhood
Severity of disease	Less	More
Lactic acidosis	More common	Not seen

Mutation Arises in mtDNA

Mixed population of wild-type and mutant mtDNA within a single cell is known as heteroplasmy. Heteroplasmic cells divide and the mtDNA is distributed randomly to daughter cells resulting in skewed population of wild-type or mutant mtDNA. Random mitotic segregation of mtDNA causes varying proportions of mutant mtDNA in daughter cells. The degree of heteroplasmy determines clinical phenotype.

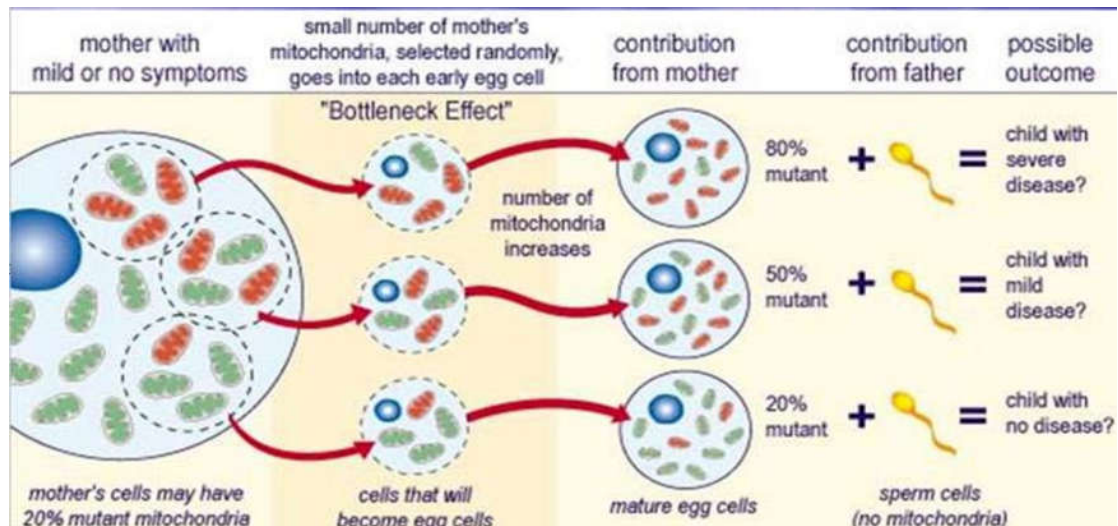


Figure 7. Maternal inheritance of mitochondrial DNA mutations.

5. Conclusions

In general real time-PCR technique can show that, in comparison to WT cells, removal of HtrA2 causes a considerable up-regulation of Hsp60 expression. This may be associated with a reduction in the threshold for mitochondrial stress in HtrA2 KO cells, which would result in an up-regulation of Hsp60 that is significantly lower in HtrA2 KO cells than in WT cells after ADEP4 and ACP5 treatment.

The transcription factor CHOP regulates mitochondrial stress signaling in cells, and in these cells, the up-regulation of Hsp60 after ADEP4 and ACP5 treatments is entirely eliminated. Both the loss of HtrA2 and the loss of CHOP appear to have a significant impact on the transcriptional activation of mitophagy as indicated by the levels of Atg5.

Funding: This research received no external funding; it is self-funded by the author.

Institutional Review Board Statement: "Not applicable" the studies are not involving humans or animals.

Informed Consent Statement: "Not applicable." the studies are not involving humans.

Conflicts of Interest: The authors declare no conflicts of interest.

References

1. Goyal, S., Chaturvedi, R.K. Mitochondrial Protein Import Dysfunction in Pathogenesis of Neurodegenerative Diseases. *Mol Neurobiol* **58**, 1418–1437 (2021). <https://doi.org/10.1007/s12035-020-02200-0>
2. Bischof, J., Salzmann, M., Streubel, M. *et al.* Clearing the outer mitochondrial membrane from harmful proteins via lipid droplets. *Cell Death Discov.* **3**, 17016 (2017). <https://doi.org/10.1038/cddiscovery.2017.16>
3. Gaziev, A.I., Abdullaev, S. & Podlitsky, A. Mitochondrial function and mitochondrial DNA maintenance with advancing age. *Biogerontology* **15**, 417–438 (2014). <https://doi.org/10.1007/s10522-014-9515-2>
4. Picca, A.; Lezza, A.M.S.; Leeuwenburgh, C.; Pesce, V.; Calvani, R.; Landi, F.; Bernabei, R.; Marzetti, E. Fueling Inflamm-Aging through Mitochondrial Dysfunction: Mechanisms and Molecular Targets. *Int. J. Mol. Sci.* **2017**, *18*, 933. <https://doi.org/10.3390/ijms18050933>
5. Temelie, M.; Talpur, R.; Dominguez-Prieto, M.; Dantas Silva, A.; Cenusa, C.; Craciun, L.; Savu, D.I.; Moiso, N. Impaired Integrated Stress Response and Mitochondrial Integrity Modulate Genotoxic Stress Impact and Lower the Threshold for Immune Signalling. *Int. J. Mol. Sci.* **2023**, *24*, 5891. <https://doi.org/10.3390/ijms24065891>
6. Celardo, I., Lehmann, S., Costa, A. *et al.* dATF4 regulation of mitochondrial folate-mediated one-carbon metabolism is neuroprotective. *Cell Death Differ* **24**, 638–648 (2017). <https://doi.org/10.1038/cdd.2016.158>

7. Puspita, L., Chung, S.Y. & Shim, Jw. Oxidative stress and cellular pathologies in Parkinson's disease. *Mol Brain* **10**, 53 (2017). <https://doi.org/10.1186/s13041-017-0340-9>
8. Garabadu, D., Agrawal, N. Naringin Exhibits Neuroprotection Against Rotenone-Induced Neurotoxicity in Experimental Rodents. *Neuromol Med* **22**, 314–330 (2020). <https://doi.org/10.1007/s12017-019-08590-2>

Disclaimer/Publisher's Note: The statements, opinions and data contained in all publications are solely those of the individual author(s) and contributor(s) and not of MDPI and/or the editor(s). MDPI and/or the editor(s) disclaim responsibility for any injury to people or property resulting from any ideas, methods, instructions or products referred to in the content.